ORBITAL DEBRIS REMOVAL BASED ON A HYBRID APPROACH COMBINING OPTIMAL CONTROL AND ENVIRONMENTAL PERTURBATIONS

Marie-Kiki Langelier(1) **and Jean de Lafontaine**(2)
(1) (2) *Université de Sherbrooke, 2500 boulevard de l'Université, Sherbrooke (QC), J1K 2R1*
(1) *Marie-Kiki.Langelier@USherbrooke.ca*
(2) *819-821-8000, ext. 62116, Jean.DeLafontaine@USherbrooke.ca*
(2) *NGC Aerospace Ltd., 1650 rue King Ouest, Bureau 202, Sherbrooke (QC), J1J 2C3, 819-348-9483, jean.delafontaine@ngcaerospace.com*

Abstract: *The orbital debris population is growing steadily year after year. Past a certain threshold, the debris density could create an uncontrolled chain reaction: the Kessler effect. To avoid this reaction, orbital debris removal in low earth orbit needs to be seriously considered. The advantageous use of environmental perturbations could reduce the propellant cost necessary for the orbital debris removal operations. This paper presents a strategy to remove orbital debris, by lowering their orbit for re-entry in Earth's atmosphere, while optimising propellant cost. Numerical simulations are realised on MATLAB/Simulink. The models include an atmospheric model (Jacchia 1977), a model of the satellite's dynamics expressed in equinoctial elements and the dominant perturbations: atmospheric drag and Earth's non-sphericity (J_2). An optimal control algorithm is also developed to compute the optimal trajectory to de-orbit the debris. This paper presents the optimal conditions in which the debris should be released for its disintegration in Earth's atmosphere, along with the propellant cost for such a mission. Two types of release orbits are analysed: circular and eccentric. It is shown that the eccentric orbit possesses advantages in terms of propellant. This paper demonstrates that it is possible to realise orbital debris removal missions while reducing the propellant cost through the advantageous use of environmental perturbations.*

Keywords: *Orbital debris removal, Optimal control, Atmospheric drag*

1. Introduction

Ever since the launch of Sputnik 1 in 1957, the exploitation of the space environment has been growing every year and the number of orbital debris has been naturally expanding. Beyond a given threshold, it is predicted that orbital debris density will create an uncontrolled chain reaction of collisions: the Kessler effect. Low-Earth Orbit (LEO) debris removal could avoid this reaction. Indeed, the greatest density of debris can be found in the LEO region, on sun-synchronous near-circular orbits of about 800 km altitude. In this study, debris removal consists in moving debris from their initial orbit to a lower release orbit leading to their disintegration in the Earth's lower atmosphere. Using orbital perturbations, it is possible to reduce the amount of propellant necessary to realise the de-orbit manoeuvres. The objective of the present study is to develop an autonomous control strategy which optimises the propellant and manoeuvre duration to modify the orbit of debris using environmental perturbations.

Many papers focusing on orbital debris removal have been produced, and all use a different method to eliminate the debris, e.g. electrodynamic tethers [1], "Ion Beam Shepherd Spacecraft" [2] or use of inflatable devices [3]. In the objective of reducing propellant cost, the method chosen for the debris removal is the use of a "space cleaner" satellite equipped with electrical propulsion. The lowering of the debris' orbit is computed through optimal control theory to optimise the propellant cost. The study focuses on the de-orbiting phase; the rendezvous and capture between the "space cleaner" and the debris are not considered.

The optimal trajectory problem using an electrical propulsion system is a well-known problem. [4] and [5] have developed optimal trajectories for such a system using equinoctial elements. However, none of them have applied this algorithm directly to a debris removal problem and used the perturbations, especially the atmospheric drag, to reduce the propellant cost.

The de-orbit trajectory which optimises fuel and time is computed using a hybrid approach combining optimal control including the J_2 perturbation and strategies that use the atmospheric drag, in particular the diurnal bulge. Depending on the position of the terminal orbit's ascending node, the spacecraft could encounter up to two times the drag force if it is situated in the bulge. Another element of this study is the analysis and comparison of two types of release orbits: circular and eccentric. The eccentric orbit manoeuvre consists of lowering the perigee in the bulge while maintaining the apogee at the original altitude (800 km in the present study). Simulations are run and validated using MATLAB/Simulink. The atmosphere model is based on an analytic version of the Jacchia 1977 model [6].

2. Nonlinear Dynamics Equations Using Equinoctial Elements and Optimal Control

Since the target orbit for debris removal is almost circular, singularities may occur if classical orbital elements are used. Therefore, the dynamics equations are expressed in terms of the equinoctial elements. The equinoctial elements, as used in the present work, are defined as:

$$\begin{aligned}
a &= a \\
h &= e \sin(\omega + \Omega) \\
k &= e \cos(\omega + \Omega) \\
p &= \tan\left(\frac{i}{2}\right) \sin \Omega \\
q &= \tan\left(\frac{i}{2}\right) \cos \Omega \\
\lambda &= M + \omega + \Omega
\end{aligned} \tag{1}$$

where $a, e, i, \omega, \Omega, M$ are the classical (Keplerian) orbital elements.

The equations defining the orbital dynamics with equinoctial elements including the J_2 perturbation are developed in [4] and [5]. The reader is referred to these references for further details. These equations are implemented in MATLAB/Simulink.

Optimal control theory, nominally the Pontryagin maximum, is used to develop an orbital transfer trajectory to de-orbit the debris. The use of optimal control theory allows the reduction of propellant cost. The optimal orbital transfer algorithm is largely based on [4] and [5]. The index to be minimised is:

$$J = \int_{t_0}^{t_f} -\frac{T^2}{2} dt \tag{2}$$

where T is the electric engine's applied force during a manoeuvre from time t_0 to t_f.

The optimal control problem leads to a two-point boundary value problem, which is solved using the shooting method. Note that in the present study, the optimal control problem is fixed-time, and the time is set so that the forces applied by the propulsion system during the manoeuvre do not exceed 70 mN. This value is based on the SMART-1 electrical propulsion system.

3. Perturbations

Since the target debris is in a Low Earth Orbit (LEO), the two main perturbations affecting the satellite's position on its orbit are the J_2 gravitational harmonic and the atmospheric drag. The optimal trajectory to de-orbit the debris into a lower release orbit, from which the debris will naturally disintegrate into the atmosphere, is computed by taking advantage of these two perturbations.

The J_2 effect on an orbit is well known and orbital dynamics equations including this perturbation are found in [4] and [5]. It is important to include the J_2 effect during the optimal trajectory computation through the optimal control algorithm because the final orbit of the debris will depend on the orbital parameter variations caused by the J_2 perturbation. The optimal control should not have to fight against this perturbation and produce forces which are not necessary and only consume more propellant.

The atmospheric drag is also important in LEO. The atmosphere dynamics is complex and difficult to model numerically with accuracy. However, an atmospheric model is necessary to determine the atmospheric density at each point of the satellite's orbit, in order to compute the atmospheric drag forces and how they act to modify the orbit. A dynamic model, which depends on time and other variables, is more precise than a static model. Of the many atmosphere models present in the literature, the Jacchia 1977 (J77) model was selected. This model contains analytical expressions which allow determining the exospheric temperature as a function of position, time, solar activity and geomagnetic activity. From this exospheric temperature, the atmospheric density is obtained through the temperature profiles, which are determined empirically or through the diffusion equation. The J77 model applies to altitudes from 70 to 2500 km so it is well-suited to a LEO debris removal problem. The analytical version of the J77 model (J77A) presented in [7] is implemented in this study.

Of the many variations present in a dynamic atmosphere model, the diurnal variations are the most interesting for this study. Every day, due to solar heating and the Earth's rotation, a density bulge in the atmosphere (a density maximum) is found in the direction of the Sun, where the atmosphere is hotter. This bulge is centred on the meridians where the local time is around 2-2:30 PM. A minimum value of the density is also found on the opposite of this bulge, around 4:00 AM every day. The atmospheric density thus depends on the latitude, local time and day of the year. The diurnal bulge causes a density of up to 2 times greater than other possible orbit orientations. Thus, placing the transfer and release orbits directly in the diurnal bulge could potentially accelerate the debris' re-entry and transfer orbit manoeuvre time. This, in turn, could reduce the propellant cost necessary to perform such a manoeuvre.

The atmospheric density also depends on the solar activity, which can be translated into the atmosphere's exospheric temperature: the higher the solar activity, the higher the exospheric temperature and the higher the density. The solar activity follows a known cycle and can thus be predicted. It might be favourable to wait until a period of high solar activity to perform the de-orbit activities. The area to mass ratio of the debris also affects the forces due to atmospheric drag; these forces could be heightened by using an inflatable device on the debris, such as a balloon. This is similar to an effect which was observed with the Echo satellite. For the Echo I satellite [8] [9], with no propulsive forces whatsoever, the orbital eccentricity was raised through resonance, which placed the satellite orbit's perigee at a lower altitude, thus accelerating its re-entry. This resonance could however be induced through propulsive actions, which is what will be done in this study.

4. Strategies for Use of the Diurnal Bulge

In this paper, the diurnal bulge is used to reduce the time required to perform the de-orbit manoeuvre and the time required for the debris to disintegrate in Earth's atmosphere, once it has been placed in its release orbit.

4.1. Release Orbit Determination

The first part of this study is to determine into which orbit type the debris should be released, i.e. circular or eccentric. The velocity at the perigee of an eccentric orbit is higher than the velocity on a circular orbit of the same size (same semi-major axis). Since the drag perturbation is proportional to the square of the velocity, the use of an eccentric orbit, with its perigee placed directly into the diurnal bulge, could potentially reduce the time needed for the debris to disintegrate into Earth's atmosphere. To determine which type of release orbit should be used, a relation between the circular and eccentric release orbits is developed, linking these two orbits into equivalent orbits in terms of disintegration (re-entry) time. Therefore, the concept of 'equivalent release orbits' refers to orbits for which the remaining orbital lifetime is the same, excluding the effect of the diurnal bulge, to be addressed in the next section. Also, the fuel cost and manoeuvre time needed to get from the original orbit to the equivalent orbits are compared.

Depending on the initial orbit's position with respect to the diurnal bulge (i.e. with respect to the Sun), the fuel cost for the transfer orbit manoeuvre could be reduced. If a substantial fuel economy is to be made, it could be advantageous to use the J_2 perturbation to drift to the desired right ascension of the ascending node. However, it is not advantageous to command a manoeuvre to the desired right ascension of the ascending node, since these manoeuvres are very costly.

4.2. Remaining Lifetime

The remaining lifetime of the debris in its release orbit could be reduced by taking advantage of the diurnal bulge. The energy loss per orbit is analysed because it presents a high variation depending on the orbit's position with respect to the Sun (MLTAN – "Mean Local Time of Ascending Node"). For different equivalent orbits, the energy loss per orbit is compared depending on the orbit's MLTAN. It is expected that orbits located in the diurnal bulge will show a greater energy loss per orbit. Developing a relation between the release orbit lifetimes and their energy loss per orbit, the lifetime which can be saved by using orbits located in the diurnal bulge can be determined.

5. Results

This section presents the different tests executed, along with results and interpretation. First, the steps required to obtain equivalent orbits (circular versus eccentric) in terms of remaining lifetime are presented. Then, it is proven that the transfer orbit manoeuvre to an eccentric release orbit is less demanding in terms of propellant than to a circular release orbit. Furthermore, the eccentric orbit allows taking greater advantage of the diurnal bulge by placing the orbit's perigee directly in the bulge. Two principal steps of the tests are defined:

1. Determination of a release orbit
    a. Determination of equivalent orbits (circular/eccentric)
    b. Cost of the transfer orbit manoeuvres (optimal control)
2. Use of the diurnal bulge to reduce remaining lifetime

5.1. Test Cases Definition

Different test scenarios have been defined, in which the parameters that vary are the atmosphere's exospheric temperature and the satellite/debris' area to mass ratio. The exospheric temperature depends on the solar activity and thus on the day of the manoeuvre's execution. In this study, the exospheric temperature is considered fixed throughout the manoeuvre. The area to mass ratio of the satellite/debris can be modified by a device which augments the drag, e.g. an inflatable balloon. Raising the area to mass ratio causes greater forces to be applied on the satellite/debris by the atmospheric drag, which accelerates its re-entry. The different test cases are presented in Tab. 1.

Table 1. Test cases definition

Test Case	**Test 1**	**Test 2**	**Test 3**	**Test 4**
Exospheric Temperature - T_∞ (K)	1000	1500	1000	1500
Area to Mass Ratio (m^2/kg)	0,04	0,04	0,4	0,4

The initial debris orbit has an altitude of 800 km, is quasi-circular ($e = 0{,}0014$) and quasi-polar sun-synchronous ($i = 98{,}6029°$). Orbits with different values for the right ascension of the ascending node are presented for comparison, since this parameter is not modified in orbit because of its high propellant cost. It could be beneficial to wait for the J_2 perturbation to naturally modify this parameter before executing the transfer manoeuvre phase. Of course, this wait implies a greater time necessary to de-orbit the debris. During the orbital manoeuvre, the argument of perigee is free to vary. An electrical engine with specific impulse of 3000 s and an initial combined mass of the "space cleaner" and debris of 1000 kg are assumed.

5.2. Release Orbit Determination

5.2.1 Equivalent Orbits

Two different types of release orbits are analysed: the circular release orbit and the eccentric release orbit. Since the start orbit is quasi-circular, getting to the circular release orbit involves a circular to circular orbit transfer. Getting to the eccentric orbit, however, involves lowering only the orbit's perigee and keeping its apogee at the initial circular orbit altitude. This section will determine the relation between the circular and eccentric release orbits so that their remaining orbital lifetime is equivalent. These orbits will then be called equivalent orbits.

Using NASA's "Debris Assessment Software" (DAS), it is possible to analyse the necessary time for a debris in a given release orbit to naturally disintegrate in Earth's atmosphere. With the DAS, the equivalent orbits can be found. For an initial circular orbit of 800 km altitude, it has been determined that each circular release orbit has an eccentric equivalent release orbit for which the perigee altitude is about 120 km below the corresponding circular orbit altitude. This relation can be observed in Fig. 1, in which the disintegration time is shown as a function of the orbit's perigee (altitude for circular orbit). Note that the DAS uses the J77 static atmosphere model, therefore not including the diurnal bulge. The exospheric temperature is computed from a solar flux table which has to be updated periodically. Figure 1 shows the orbit lifetime as a function of the perigee/circular orbit altitude. In this figure, the solid lines represent the circular orbits while the dotted lines represent the eccentric orbits. The "120 km rule" can be deduced from this figure. Figure 2 shows more clearly the 120 km difference between the perigee altitude of the eccentric orbit and the altitude of the circular orbit by plotting the equivalent orbits' altitude difference as a function of remaining lifetime. Note that this "120 km rule" only applies to eccentric orbits with an 800 km altitude apogee. For a different apogee altitude, a new rule would have to be developed. According to the DAS, the "120 km rule" is independent of the exospheric temperature, i.e. of the date at which the simulation is run.

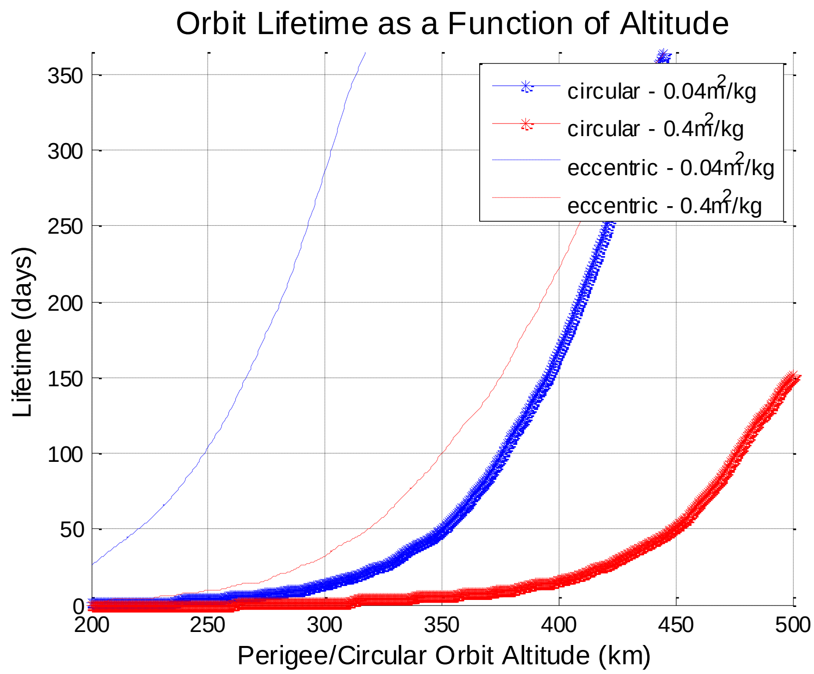

Figure 1. Orbit Lifetime as a Function of Altitude

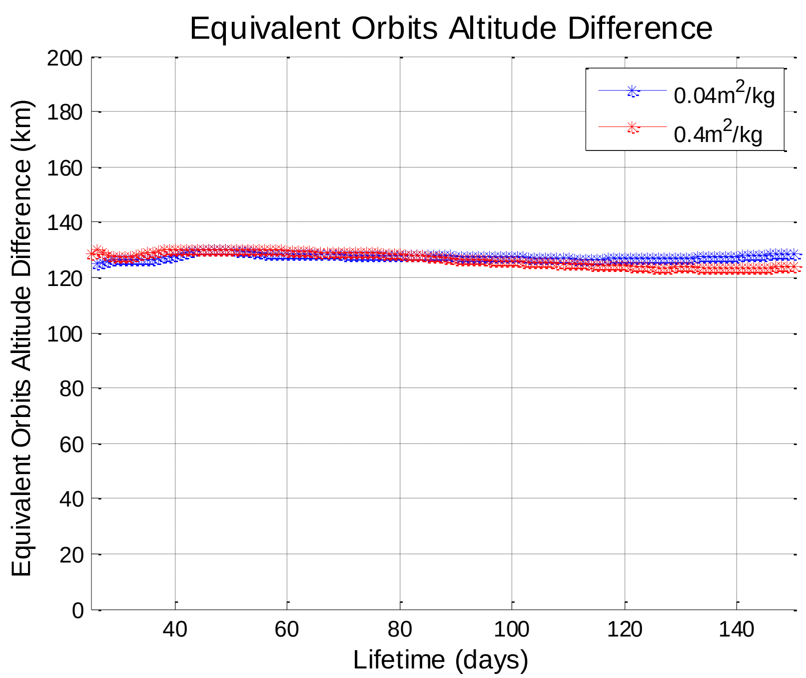

Figure 2. Equivalent Orbits Altitude Difference

Following the “120 km rule”, the equivalent orbits which are of interest in this study are presented in Tab. 2.

Table 2. Equivalent Orbits

Circular Orbit	Eccentric Orbit
300x300 km	800x180 km
350x350 km	800x230 km
400x400 km	800x280 km
450x450 km	800x320 km
500x500 km	800x380 km

5.2.1 Transfer Orbit Manoeuvre Analysis

The fuel-optimal trajectories to get to the equivalent release orbits are found using optimal control theory, including the J_2 perturbation. This optimal control is then fed into the open-loop simulator (MATLAB/Simulink) including J_2 and atmospheric drag (including diurnal bulge) perturbations. The radial and normal controls, computed by the guidance law, oscillate around zero. They are forced to zero, keeping only the transverse force which allows modifying the orbit's semi-major axis and eccentricity. This avoids spending additional fuel to correct for effects that are null when they are averaged over the total orbital manoeuvre. It is also assumed that the manoeuvres are performed at the spring equinox, while the orbital plane is in the bulge and an argument of perigee value of zero corresponds to the middle of the diurnal bulge. At the start of the manoeuvre, the argument of perigee is located in the middle of the diurnal bulge ($\omega = 0$) and MLTAN = 0. The results are presented below, in Fig. 3 and Fig. 4, where the solid lines represent the circular release orbits and the dotted lines represent the equivalent eccentric release orbits.

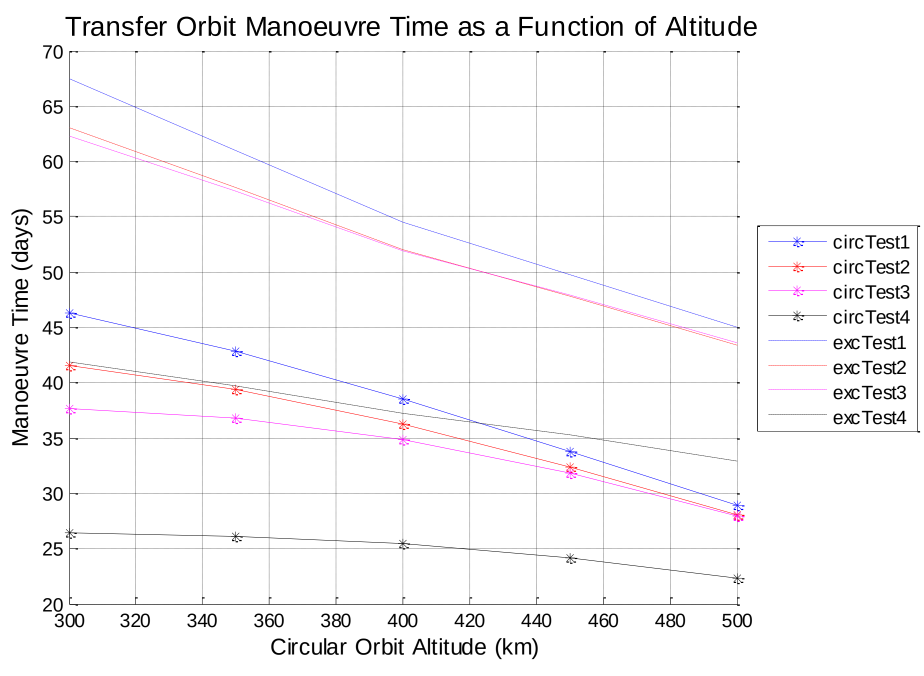

Figure 3. Transfer Orbit Manoeuvre Time as a Function of Altitude

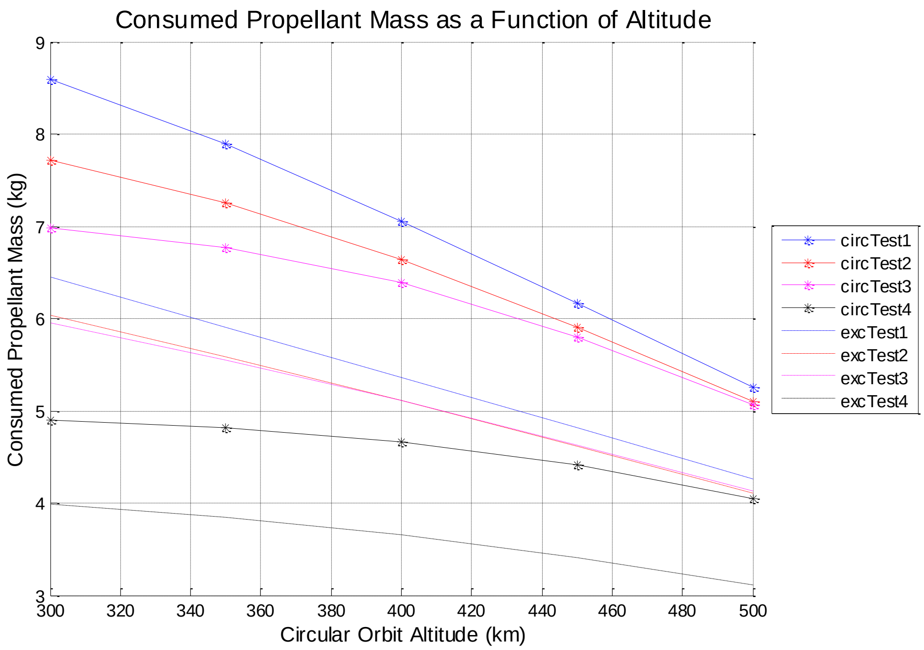

Figure 4. Consumed Propellant Mass as a Function of Altitude

Summarising, the manoeuvre to reach the eccentric release orbit takes around 49% more time to realise but results in about 21% propellant savings. The results are independent of the test scenario and the perigee altitude. There is thus a propellant mass advantage in using an eccentric release orbit if manoeuvre time is not critical.

The fuel-cost advantage of the eccentric release orbit is also augmented when the diurnal bulge in the density of the atmosphere is considered. For each circular and eccentric release orbit, a different initial MLTAN (different right ascension of the ascending node) will induce different orbital geometries with respect to the diurnal bulge. The geometries that place the perigee in the bulge will bring an additional advantage during the transfer orbit manoeuvre. This effect is seen on the Fig. 5 for the particular test case number 4. The solid lines illustrate fuel cost to reach the circular release orbits and the dotted lines illustrate the fuel cost for the equivalent eccentric release orbits.

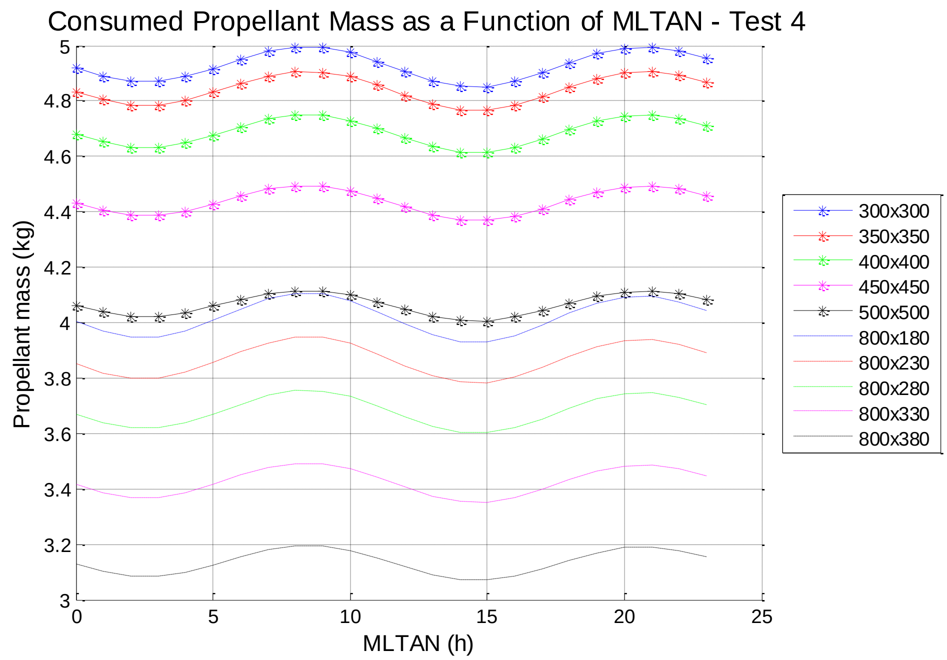

Figure 5. Consumed Propellant Mass as a Function of MLTAN During Transfer - Test 4

Test case number 4 is most affected by the diurnal bulge. This test case combines a high exospheric temperature and a high area to mass ratio. This test scenario is thus most affected by the diurnal bulge variations and the starting MLTAN can affect the propellant mass necessary to get to the release orbit. To consult the results for the other test cases, please refer to [10].

5.3. Remaining Lifetime

It has been shown in Fig. 5 that the initial MLTAN of the transfer orbit modulates the fuel cost required to reach the equivalent release orbits, because of the diurnal bulge. The effect of the diurnal bulge (thus MLTAN) on the orbital lifetime once the debris is in its release orbit is now assessed. The specific energy loss per orbit (deltaE) is a measure of the rate of loss of orbital energy and is used here as an indicator of the effects of the diurnal bulge. For the "120 km rule" to apply to the energy loss per orbit, a relation between the remaining orbit lifetime and energy loss has to be developed. This relation depends on the altitude of the circular orbit and the exospheric temperature. Figure 6 presents, for the different test cases, the ratio between the energy losses per orbit of the equivalent circular and eccentric release orbits as a function of the perigee/circular orbit altitude. Recall that, because of their equivalence, the eccentric and the corresponding equivalent circular release orbits both have the same remaining orbital lifetime. It can be noticed that the mean energy loss for the eccentric orbit is always higher than that of the circular orbit, which is to be expected since the eccentric orbit has a larger semi-major axis and thus has more energy to lose until reaching the same re-entry conditions. Also, the higher the circular orbit altitude, the lower the ratio between the eccentric and circular orbits. There is thus a greater advantage in using an eccentric orbit when its perigee altitude is lower. Raising the exospheric temperature also implies a decrease in this ratio. For a circular orbit of 300 x 300 km, test cases 1 and 3 ($T_{\infty} = 1000\ K$) imply an eccentric orbit with an energy loss per orbit about 3.9

times greater than that for the circular orbit, while test cases 2 and 4 ($T_\infty = 1500\ K$) imply an eccentric orbit with an energy loss per orbit about 2.25 times greater than that of the circular orbit. Raising the exospheric temperature by 500 K, the ratio between the eccentric and circular release orbits' energy loss per orbit has been reduced by a factor 1.73. Note that test cases with the same exospheric temperature but different area to mass ratios (Test1-Test3 and Test2-Test4) are equivalent when computing these ratios. The area to mass ratio of the circular and eccentric equivalent orbits are equal, thus when computing the energy loss per orbit ratio, they cancel each other out.

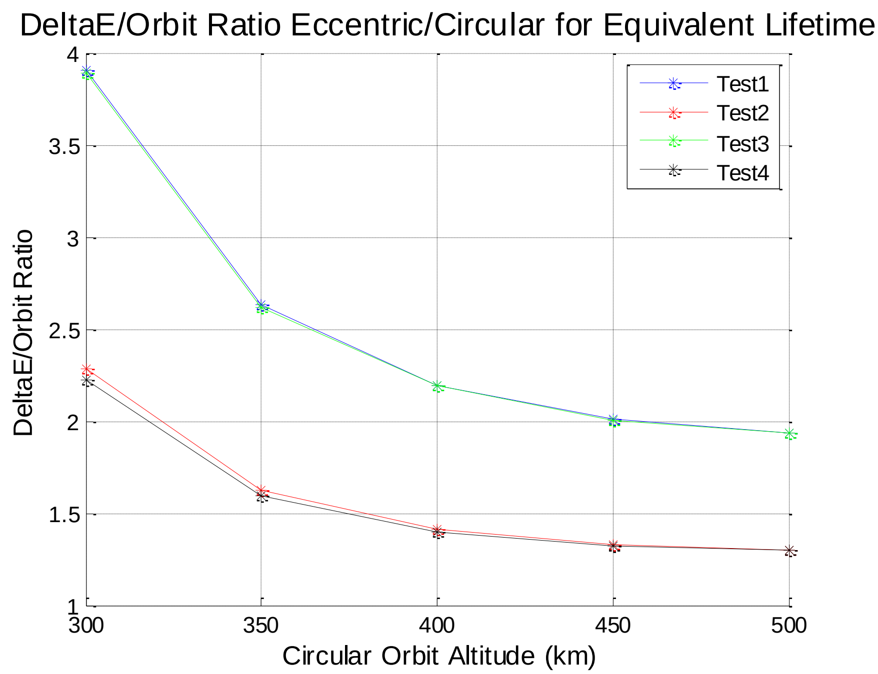

Figure 6. DeltaE/orbit Ratio Eccentric/Circular for Equivalent Lifetime

The energy loss per orbit is now used to assess the effect of the diurnal bulge. The energy loss per orbit is plotted as a function of the orbital plane orientation with respect to the Sun (MLTAN). The eccentric release orbit always loses more energy per orbit than its equivalent circular orbit, independently of its position with respect to the Sun. This result is expected since the eccentric orbit has a greater semi-major axis than the circular orbit, thus it has more orbital energy to dissipate for the same lifetime and this translates into a greater required energy loss per orbit. As indicated earlier, the diurnal bulge of the atmosphere will modulate the energy loss per orbit, particularly for the eccentric orbit, and thus, it will modulate the lifetime. The optimal release orbit corresponds to an eccentric orbit with its perigee located in the diurnal bulge. This orbit would allow for the fastest re-entry of the debris in Earth's atmosphere. Figure 7 shows these results, for the equivalent orbits, as a function of the position of the debris orbit with respect to the Sun (MLTAN), assuming that it is the spring equinox (March 21). Note that a logarithmic scale has been used to enable a clear view of the different curves.

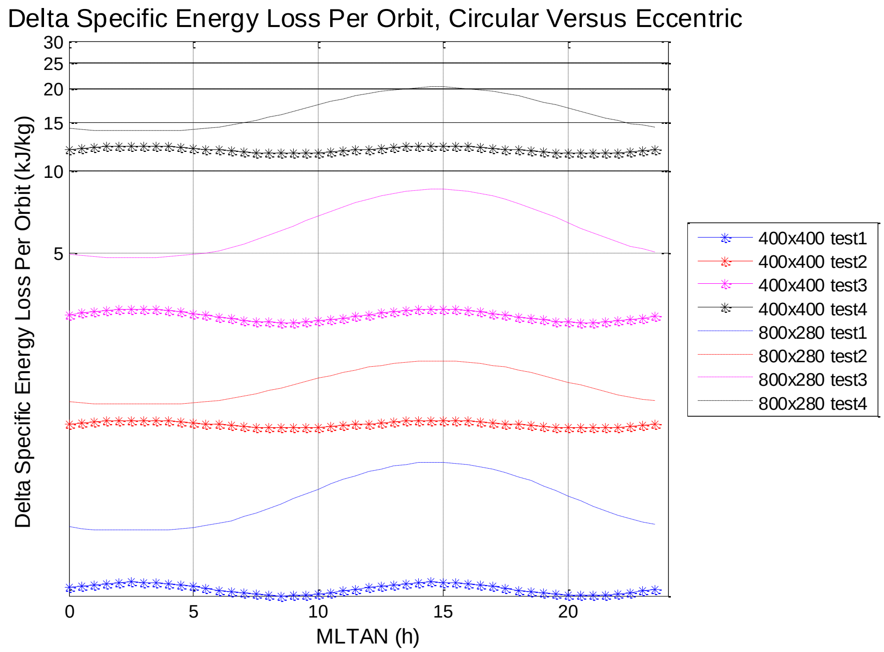

Figure 7. Delta Specific Energy Loss per Orbit Circular Versus Eccentric

For an eccentric orbit, it is seen on Fig. 7 that when the perigee is located directly in the atmosphere's diurnal bulge, that is when MLTAN is around 14-15 h and the argument of perigee is zero, the maximum energy loss is obtained. Inversely, the minimum energy loss is obtained when the perigee is located at the opposite of the diurnal bulge. However, in this situation, the argument of perigee could be controlled to 180° instead of 0°, taking full advantage of the diurnal bulge. In general, since the argument of perigee is an orbital element that is easy to modify through manoeuvres compared to the right ascension of ascending node (equivalent to MLTAN), which is constrained by the original orbit of the debris, the position of the perigee in the orbital plane can always be tuned to maximise the energy loss per orbit in accordance with Fig. 7. For the equivalent circular release orbits, the MLTAN modulation caused by the diurnal bulge is less apparent, as expected. The debris goes through the diurnal bulge on half of its orbit, even if the argument of perigee is 0° or 180°.

Finally, the variation in energy loss per orbit caused by the MLTAN and the choice of the argument of perigee is now translated into difference in remaining orbital lifetime. The orbital lifetime is plotted as a function of the mean energy loss per orbit. Note that the orbit lifetime has been computed with the NASA DAS software. These figures allow determining the lifetime which can be saved by using orbits located in the diurnal bulge. By comparing the lifetime for an orbit located in the diurnal bulge (maximum energy loss per orbit) to the lifetime of the same orbit located at its minimum energy loss per orbit, a lifetime difference is obtained. Figure 8 shows these differences as a function of the circular orbit's altitude. The most advantageous lifetime difference is found for the eccentric release orbits of test cases 1 and 2 (no inflatable device to raise the atmospheric drag). When the atmospheric drag is raised by the use of an inflatable device, there is a smaller difference between the lifetime of the orbit in the bulge and the one out of the bulge. The figure also shows that the eccentric release orbits (dotted lines) always offer a better option than the circular release orbits (solid lines) to take advantage of the diurnal bulge. Also, a lower exospheric temperature slightly allows taking better advantage of the diurnal bulge (in terms of saved lifetime with respect to the minimum energy loss per orbit).

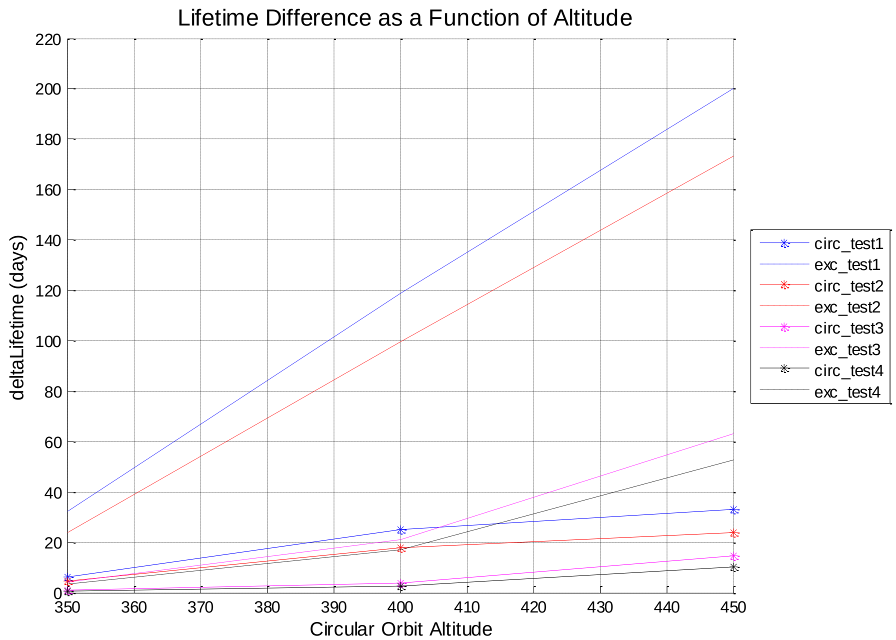

Figure 8. Lifetime Difference as a Function of Altitude

6. Conclusion

This paper has shown that environmental perturbations can be used advantageously for orbital debris removal manoeuvres. The atmospheric drag, especially the diurnal bulge, has been used to reduce the propellant cost and manoeuvre time of a debris removal manoeuvre. An eccentric release orbit with its perigee located directly in the diurnal bulge offers the greatest advantage in terms of propellant cost.

As future work, instead of computing the remaining lifetime which can be saved by using the diurnal bulge, one could compute the propellant mass which could be saved by de-orbiting to a higher perigee release orbit.

7. Acknowledgements

The author wishes to acknowledge the financial support of the Natural Sciences and Engineering Research Council of Canada (NSERC).

8. References

[1] Kawamoto, S., Makida, T., Sasaki, F., Okawa, Y. and Nishida, S. (2006). Precise numerical simulations of electrodynamic tethers for an active debris removal system. Acta Astronautica, volume 59, no. 1-5, p. 139-148.

[2] Bombardelli, C. and Pelaez, J. (2011). Ion Beam Shepherd for Contactless Space Debris Removal. Journal of Guidance, Control, and Dynamics, volume 34, no. 3, p. 916-20.

[3] Lücking, C., Colombo, C. and McInnes, C. (2011). A Passive De-orbiting Strategy for High Altitude CubeSat Missions using a Deployable Reflective Balloon. 8th IAA Symposium on Small Satellites, 2011-04-04 - 2011-04-08, Berlin.

[4] Kechichian, J.A. (1996). Optimal low-thrust rendezvous using equinoctial orbit elements. Acta Astronautica, volume 38, no. 1, p. 1-14.

[5] Tarzi, Z., Speyer, J. and Wirz, R. (2013). Fuel optimum low-thrust elliptic transfer using numerical averaging. Acta Astronautica, volume 86, May-June 2013, p. 95-118.

[6] Jacchia, L.G. (1977). Thermospheric temperature, density, and composition: new models. Smithsonian Astrophysical Observatory, Special Report 375.

[7] De Lafontaine, J. and Hugues, P. (1983). An Analytic Version of Jacchia's 1977 Model Atmosphere. Celestial Mechanics, volume 3, no. 26.

[8] Buckingham, A.G., Lim, Y.C. and Miller, J.A. (1965). Orbit position control using solar pressure. Journal of Spacecraft and Rockets, volume 2 no. 6, p. 863-867.

[9] Jones, H.M. et Shapiro, I.I. (1960). Effects of solar radiation pressure on earth satellite orbits. Science, volume 131, no. 3404, p. 920-921.

[10] Langelier, M.-K. (2015). Commande optimale d'un satellite à propulsion électrique utilisant les perturbations pour l'élimination des débris orbitaux en basse altitude, Master's thesis, Université de Sherbrooke. In preparation.